

Size Effects on the Bending Behaviour of Reinforced Concrete Beams

Brincker, Rune; Henriksen, M. S.; Christensen, F. A.; Heshe, Gert

Published in:
Minimum Reinforcement in Concrete Members

Publication date:
1999

Document Version
Publisher's PDF, also known as Version of record

[Link to publication from Aalborg University](#)

Citation for published version (APA):
Brincker, R., Henriksen, M. S., Christensen, F. A., & Heshe, G. (1999). Size Effects on the Bending Behaviour of Reinforced Concrete Beams. In A. Carpinteri (Ed.), *Minimum Reinforcement in Concrete Members: ESIS Publication 24* (pp. 127-137). Pergamon Press.

General rights

Copyright and moral rights for the publications made accessible in the public portal are retained by the authors and/or other copyright owners and it is a condition of accessing publications that users recognise and abide by the legal requirements associated with these rights.

- Users may download and print one copy of any publication from the public portal for the purpose of private study or research.
- You may not further distribute the material or use it for any profit-making activity or commercial gain
- You may freely distribute the URL identifying the publication in the public portal -

Take down policy

If you believe that this document breaches copyright please contact us at vbn@aub.aau.dk providing details, and we will remove access to the work immediately and investigate your claim.

SIZE EFFECTS ON THE BENDING BEHAVIOUR OF REINFORCED CONCRETE BEAMS

R. BRINCKER, M.S. HENRIKSEN, F.A. CHRISTENSEN and G. HESHE,
*Aalborg University, Sohngaardsholmsvej 57,
9000 Aalborg, Denmark*

ABSTRACT

Load-deformation curves for reinforced concrete beams subjected to bending show size effects due to tensile failure of the concrete at early stages in the failure process and due to compression failure of the concrete when the final failure takes place. In this paper these effects are modelled using fracture mechanical concepts, and size effects of the models are studied and compared with experimental results.

KEYWORDS

Size effect, bending behaviour, reinforced concrete, minimum reinforcement, rotational capacity, fracture mechanics.

INTRODUCTION

The considered problem is the bending behaviour of simply supported concrete beams, Figure 1. The basic variables are the beam geometry given by the width b , the depth h and the span l , the concentrated load F acting at the middle of the beam and the corresponding displacement u .

The bending response of the beam is described by the load-deflection curve, Figure 1, depicting the loading force F as a function of the displacement u .

It is assumed, that the parameters influencing the bending response of the beam, apart from the basic parameters mentioned above, are the concrete type described by Young's Modulus E and the softening relations in tension and compression, the reinforcement type given by the stress-strain relation for the steel and the shear friction stress τ_f for the debonding, the reinforcement ratio φ , the number of re-bars n and the placement of the re-bars as given by the distance h_{ef} from the top of the beam. Note, that no softening relation is considered for the reinforcement. Thus, in this analysis, the contribution from necking of the re-bars, is neglected.

At early stages of the failure process, the response is governed by the tensile properties of the concrete, the elastic properties of the reinforcement steel, and the debonding process between concrete and steel. Typically, the response will show a local force maximum F_i where the concrete

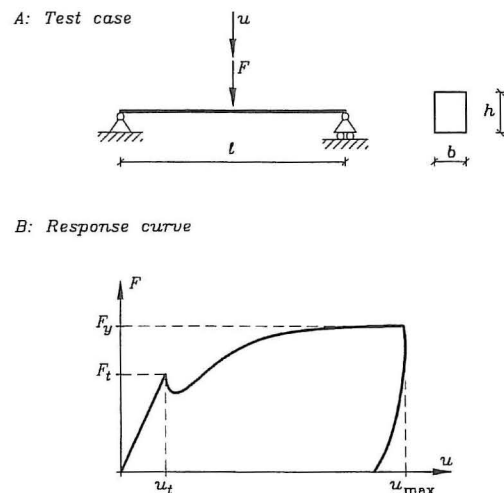


Figure 1. Fundamental problem of the investigation. A: The test case, B: Response curve.

starts cracking, a decrease afterwards, and then a slowly increasing response as the reinforcement starts debonding taking over the stresses relieved by concrete tensile failure. Later, when the tensile stresses in the concrete have decreased to zero, and yielding of the reinforcement bars is fully developed, the response curve reaches a nearly constant value F_y . For convenience, here F_y is just defined as the maximum value of the response in the "yielding regime".

Since concrete tension failure is highly size dependent, the first part of the response curve will show strong size effects. For large beams, the concrete contribution will be small and brittle compared to smaller beams, meaning that the ratio F_t/F_y will be size dependent. Thus, the ratio F_t/F_y is a central parameter for description of the size effects at early stages of the failure process. It describes, one can say, the size effect on the load scale. In most standards, the minimum reinforcement requirements aim at keeping this ratio below a certain value, securing a ductile behaviour of the beam in load control. Therefore, size effects at early stages of the failure process are closely associated with the minimum reinforcement issue.

In the first main section of this chapter, size effects on the load scale are studied under different assumptions using a non-linear fracture mechanical model for the tension failure of the concrete, and a simple friction model for the reinforcement debonding. Size effects on the bending response are studied for constant reinforcement ratios and constant values of Carpinteri's brittleness number.

When studying size effects on the late stages of the failure process, it is necessary to focus on the deformation scale. Thus, it might seem natural to choose a corresponding set of displacement parameters u_t and u_{max} , see Figure 1, and then define the corresponding ratio as the key parameter. However, since both displacements are influenced by the elastic response of the beam, in this chapter a non-dimensional parameter θ describing size effects on the displacement scale is defined

by the work equation

$$\theta M_y = \int_0^\infty F du \quad (1)$$

where M_y is the yield moment corresponding to the yield force F_y . Now, using the simple relationship $M_y = \frac{1}{4} F_y l$, the parameter θ is given by

$$\theta = \frac{4}{l} \int_0^\infty \frac{F}{F_y} du \quad (2)$$

As it appears, the integral has the dimension of length, describing the total plastic deformation of the beam. This measure is not influenced by elastic contributions and is non-sensitive to the tension failure behaviour of the concrete as long as the contribution to the area under the response curve is small.

The geometric interpretation of the parameter θ is the total concentrated rotation at the yielding section under the loading force. Thus, it is a measure of the rotational capacity of the beam.

In the last main section of this chapter, size effects on the rotational capacity of concrete beams are studied using a semi-classical approach for the lightly reinforced case, where the rotational capacity is controlled by the number of cracks in the tension side of the beam, and using a fracture mechanical approach for the heavily reinforced regime, where the rotational capacity is controlled by compression failure in the concrete.

In the following model results are compared with experimental results from a large number of tests on concrete beams of different sizes, different types of concrete (normal strength, high strength), and different reinforcement ratios. The experimental results are described in Appendix A.

MINIMUM REINFORCEMENT

A commonly accepted idea behind minimum reinforcement requirements has for a long time been that the load corresponding to tension failure of the concrete F_t should be smaller than the load-bearing capacity F_y of the cracked beam section, thus

$$F_y > F_t \quad (3)$$

Now, approximating F_t by the bending strength, according to a Navier distribution of the stresses (not a good approximation) and neglecting the reinforcement contribution, yields $F_t \frac{l}{4} = f_t \frac{1}{6} b h^2$ where f_t is the tensile strength of the concrete. Using the approximate formula for the load-bearing capacity of the cracked beam section $F_y \frac{l}{4} = k h A_s f_y$, where k is a factor typically in the range 0.8 – 0.9, and defining the reinforcement ratio as usual by $\varphi = A_s/A_c$, Equation (3) can then be written as

$$\varphi > \frac{1}{6k} \frac{f_t}{f_y} = \varphi_{min} \quad (4)$$

This might be seen as the background for most minimum reinforcement requirements in the codes. The requirement states that, for a certain choice of steel and concrete, the reinforcement ratio should just be chosen larger than a certain value. This kind of classical reinforcement criteria are investigated in detail in the following subsection.

The weakness of the classical kind of reinforcement criteria is the simplicity of the Navier type of bending strength that does not include any size effects. Thus, using the criterion (4) in practice a value for the tension strength f_t must be used that somehow includes the size effect. Usually this is done by using a value of the tensile strength estimated from bending tests on moderate size beams. A totally different approach would be to express a criterion for stable crack growth across a reinforced concrete section. Using linear fracture mechanics and some simplifications, this leads to a criterion of the type

$$N_P > N_{\min} \quad (5)$$

where N_P is Carpinteri's brittleness number for reinforced concrete

$$N_P = \frac{f_y \sqrt{h}}{K_{Ic}} \varphi \quad (6)$$

and where K_{Ic} is the fracture toughness of the concrete. In the second subsection, the criterion given by (5) is investigated assuming that the fracture toughness can be approximated by $K_{Ic} = \sqrt{EG_F}$.

Both the classical reinforcement criterion given by Equation (4), and the fracture mechanical criterion given by Equation (5) are investigated by simulating the failure responses using a fictitious crack model for the concrete failure and a pure frictional model for the reinforcement-concrete debonding, and finding the minimum values of the reinforcement ratio φ and the brittleness number N_P corresponding to fulfilment of Equation (3).

Classical Requirements for Minimum Reinforcement

The classical requirements for minimum reinforcement are investigated by simulating the failure response of beams of different size using a fictitious crack model for the concrete tension failure and a friction model for the reinforcement-concrete debonding. Details of the investigation are given in Appendix B.

Three different concretes are considered: a normal strength concrete with linear softening, a normal strength concrete with bi-linear softening, and a high strength concrete with bi-linear softening. The softening relations are shown in Figure 5 in Appendix B.

The size of the "valley" on the response curve often seen in experimental results, occurring just after the local maximum F_t corresponding to the concrete tension failure, is totally controlled by the shear friction stress τ_f . In the limit where the shear friction stress becomes infinite, the response follows a "master curve", and cases with a finite shear friction stress appear as deviations from this curve, Figure 4, Appendix B. In the simulations, the shear friction stress was chosen as $\tau_f = 5 \text{ MPa}$ for all cases, a typical value reported in the literature for ribbed reinforcement.

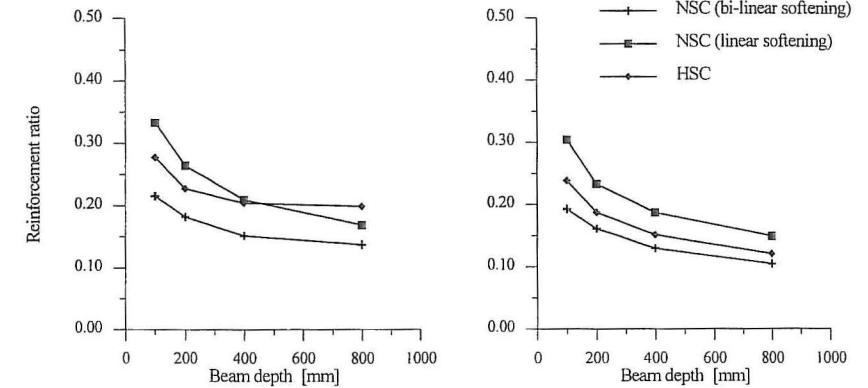


Figure 2. Reinforcement ratios corresponding to $F_y = F_t$ for different beam sizes and different softening relations. Left: No initial crack. Right: Initial crack with a depth of 7.5 % of the beam depth.

Using the simulation model so defined, the minimum reinforcement ratio φ corresponding to the smallest ratio that satisfies the overall static requirement given by Equation (3) is determined for different beam sizes. The results are shown in Figure 2. The diagrams show the results for two cases: the case of no initial crack, and the case where an initial crack is present with an initial depth of 7.5 % of the beam depth.

As it appears from the results, the reinforcement ratio corresponding to $F_y = F_t$ is clearly dependent upon the size of the beam as well as the type of softening relation. The minimum reinforcement ratio (for this type of steel) is in range 0.20 – 0.35 for very small beams reducing to 0.10 – 0.20 for large beams. Further, as expected, high strength concrete requires a higher minimum reinforcement than normal strength concrete, and a more ductile softening curve (the linear softening relation for the normal strength concrete has the same tensile strength and the same critical crack opening) requires a higher minimum reinforcement.

There is also an influence of the initial crack. As it appears, with an initial crack the minimum reinforcement ratio is less sensitive to the type of softening relation, and there is an overall tendency for the required minimum reinforcement ratio to become smaller. The presence of initial cracks does not seem to influence the size effect too much, although there seems to be a little less size effect in the case of initial cracks.

The overall result is that a unique minimum reinforcement ratio is difficult to define since the ratio corresponding to $F_y = F_t$ varies considerably. However, there are at least two important arguments in support of the simple criterion $\varphi > \varphi_{\min}$.

First, as the results clearly indicate, if a minimum reinforcement ratio φ_{\min} has been determined from bending tests on small beams, it will be on the safe side to use the criterion $\varphi > \varphi_{\min}$ on

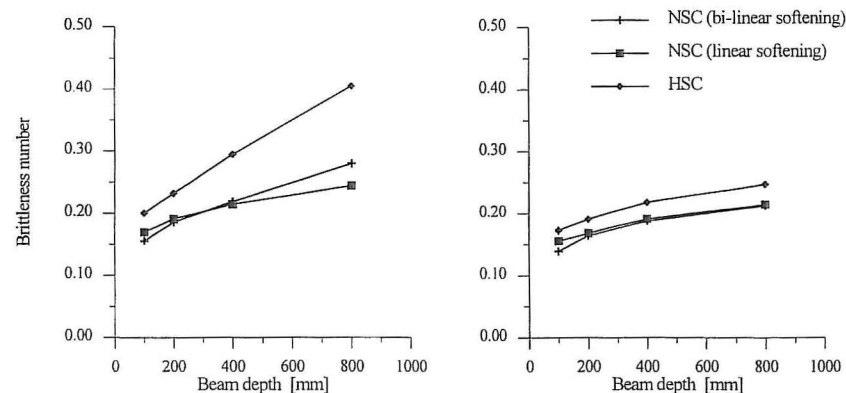


Figure 3. Carpinteri's brittleness number for reinforced beams corresponding to $F_y = F_t$ for different beam sizes and different softening relations. Left: No initial crack. Right: Initial crack with a depth of 7.5 % of the beam depth.

larger beams.

The second argument is a little more delicate, but in fact even more important. If the length scale of the softening relation is scaled with the size of the structure, i.e. if the shape of the relation is constant, and if the critical crack opening $w_c = \alpha_1 h$, where α_1 is a constant and h stands for the size of the structure, then the failure response curve (the $F-u$ curve) is shape invariant, and thus, the reinforcement ratio corresponding to $F_y = F_t$ becomes size independent. Now, a good question is, if it is reasonable to assume something like $w_c = \alpha_1 h$ in practice. It might very well be a reasonable assumption since the maximum aggregate size d_{\max} typically increases with the size of the structure, and as an average it might be reasonable to assume $d_{\max} = \alpha_2 h$. Further, micro mechanical considerations as well as some experimental results support the approximate relation $w_c = \alpha_3 d_{\max}$. Thus, in practice taking into account the typical application of larger aggregate sizes in larger structures, the reinforcement ratio that corresponds to $F_y = F_t$ will be less size-dependent than indicated by the results of this investigation.

Carpinteri's Brittleness Number

Application of Carpinteri's brittleness number is investigated in a similar way by determining the smallest value of the brittleness number that gives a simulated response curve satisfying the overall static requirement given by Equation (3). Details are given in Appendix B. The results of the investigation are shown in Figure 3.

The overall impression is that there is a size effect on Carpinteri's brittleness number. The brittleness number increases with the beam size. This is to be expected, since the square root size dependence is the strongest possible dependence corresponding to the linear fracture mechanical

case. The tensile bending problem is known to be influenced by fracture mechanical non-linearities leading to a weaker influence of the size than predicted by the brittleness number. Thus, when the minimum reinforcement ratio is corrected by a square root factor, it is to be expected that this will over-correct the size effect on the minimum reinforcement ratio, and therefore, the brittleness number becomes size depending itself.

As it appears, there is a large difference between the case of no initial crack, and the case of an initial crack. In the case with no initial crack, there is a relatively strong size effect on the brittleness number, whereas this size effect is significantly smaller in the case of an initial crack. In the case of an initial crack, the size effect on the brittleness number is smaller than the size effect on the reinforcement ratio. Thus, since initial cracks must be assumed to be present in real structures, it seems that the brittleness number for this reason might be a better choice for minimum reinforcement requirements than the reinforcement ratio.

On the other hand, a critical brittleness number found from tests on small beams will lead to results for minimum reinforcement on large beams that are on the unsafe side.

Further, it seems like the brittleness number is less sensitive to the shape of the softening relation, but depends more on the strength level of the concrete.

ROTATIONAL CAPACITY

In the lightly reinforced regime, the rotational capacity is controlled by the number of cracks and the local debonding and yielding of the reinforcement around each crack. If no debonding takes place (case of infinite shear friction stress τ_f), the length over which yielding takes place tends to zero, and thus, the contribution from yielding of the reinforcement tends to zero. In this case however, the number of cracks becomes large and thus, so does the contribution to the total work from the cracking of the concrete. In the extreme case of a very small friction stress, only one crack develops, and thus, yielding of the reinforcement is mainly responsible for maintaining the rotational capacity. These effects are described in the next subsection.

In the heavily reinforced regime, the rotational capacity is controlled by the compression failure of the concrete. A large part of the rotational capacity might come from plastic deformations of the reinforcement steel, but the deformation capacity of the concrete is the limiting parameter. If the concrete has a small deformation capacity the contribution from the plastic deformation of the reinforcement as well as the contribution from the concrete itself becomes small. The rotational capacity of heavily reinforcement beams is studied in the second subsection using a fracture mechanical approach for the compression failure of the concrete.

Lightly Reinforced Beams

In this case a semi-fracture mechanical approach is used. The location of cracks and the number of cracks are determined by a classical approach, i.e. the concrete cracks when the tensile strength is reached, and the response (the $F-u$ curve) is calculated assuming a constant shear friction stress over the debonded area. Once the response is determined, the rotational capacity is determined as described by Equation (2). A semi-fracture mechanical approach is introduced by adding the energy dissipated in the tensile cracks to the total work determined as the integral of the simu-

lated response (classical contribution). The energy dissipated in the tensile cracks is estimated as $nA_c G_F$ where n is the number of cracks. Thus, the model assumes the cracks to be fully opened and the cracks to extend approximately over the whole beam area A_c . Details are given in Appendix C.

Using a model like this, the rotational capacity is strongly dependent on the strain hardening of the reinforcement. If the strain hardening is small, yielding takes place only over a small length of the re-bars around each crack, and the only way of extending the yield length of the re-bars, is to increase the strain hardening of the steel, i.e. the ratio f_u/f_y where f_u is the ultimate failure stress of the reinforcement. This effect is shown in Figure 3 in Appendix C.

Another important main result is that the model does not show a so strong dependency on the shear friction stress τ_f as one would expect, Figure 4 in Appendix C. This is due to the semi-fracture mechanical approach where the increasing values of τ_f reduce the contribution from yielding of the reinforcement, but at the same time increase the contribution from the energy dissipation in the tensile cracks.

Figure 4 shows the size effects for two different values of the shear friction stress τ_f . If the shear friction stress has a small or moderate value (left part of Figure 4) then the number of cracks is moderate too, and the influence from the tensile failure on the rotational capacity is small. In this case, the rotational capacity is dominated by the classical contributions from yielding and frictional debonding which does not show size effects, and thus, the size effect is small. However, if the shear friction stress becomes large (right part of Figure 4), the number of cracks increases, and so does the contribution to the rotational capacity from dissipation of energy in the tensile cracks. Thus, since this contribution is size dependent, the total rotational capacity becomes size dependent. As it appears from the results, the shear friction stress has to be very large in order to enforce a size effect of importance, and even in that case, the size effects are still moderate.

Figure 6 in Appendix C shows the rotational capacity for the two different ribbed reinforcement types used in the experimental investigation, a high deformation capacity type, and a low deformation capacity type. In this case the shear friction stress is taken as $\tau_f = 5 \text{ MPa}$. As expected, size effects are small for both types of reinforcement, and the deformation capacity of the reinforcement has a large influence on the rotational capacity of all beams.

Heavily Reinforced Beams

For this case a fracture mechanical description of the compression failure is used. The main argument for this is that experimental results show that the post-peak behaviour including the post-peak energy dissipation is relatively independent of the length of a compression specimen, see Figure 2 in Appendix D.

Naturally, this leads to an assumption of localized compression failure, thus, compression failure is assumed to take place over a certain length of the compression zone. This length is denoted the characteristic length l_{ch} . The characteristic length is assumed to be proportional to the depth of the compression zone corresponding to a compression-shear failure mode with the development of slip-planes at a certain angle to horizontal. In this case the characteristic length becomes proportional to the depth h_c of the compression zone $l_{ch} = \beta h_c$. Assuming an inclination angle of the slip-planes similar to the cone-failure of a cylinder in compression, justifies the expectation of β having a value around 4.

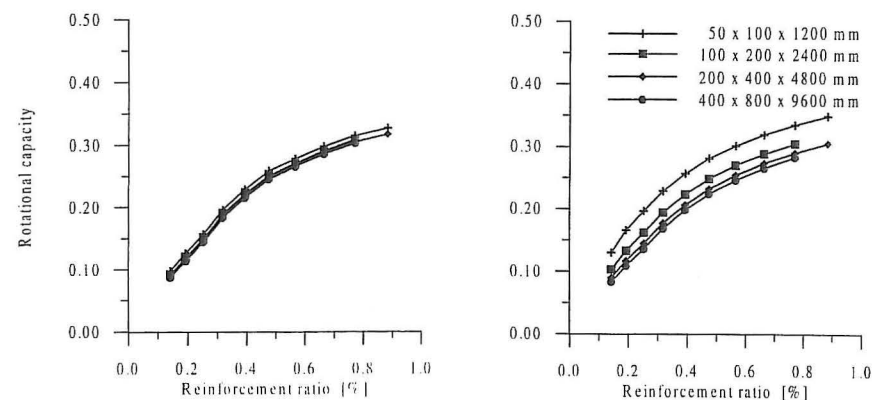


Figure 4. Size effects on the rotational capacity in the lightly reinforced regime for different values of the shear friction stress τ_f . Left: Shear friction stress $\tau_f = 5 \text{ MPa}$. Right: Shear friction stress $\tau_f = 20 \text{ MPa}$.

The model assumes a simple linear softening relation, so the model has two main parameters: the inclination parameter β , and the critical deformation w_c of the concrete in the compression failure zone.

The model is roughly calibrated by simulating failure responses of beams, calculating the rotational capacity according to Equation (2) and comparing with the experimental results for normal strength concrete. It turns out that in order to have reasonable agreement with the experimental results, the values of the key parameters of the model have to be chosen as $w_c \cong 4 \text{ mm}$, $\beta \cong 8$. These values are somewhat higher than expected, but the rather high values might be interpreted as a consequence of the loading arrangement for the tests where the loading plate used for distribution of the concentrated load might act as confinement.

In Appendix D a simple model for tension failure of the reinforcement was included in order to check if the model showed a reasonable switch between concrete compression failure and reinforcement tension failure. Results for pure compression failure are shown in Figure 5.

As it appears, the model shows a clear size effect on the rotational capacity, the rotational capacity becoming significantly smaller with increasing beam size. Further, for all beam sizes, the rotational capacity predicted by the model decreases with the reinforcement ratio. The influence from both the size and the reinforcement ratio is rather large. Thus, for high values of the reinforcement ratio, the rotational capacity is small for all beam sizes, and for the large beams, the rotational capacity is small also for moderate values of the reinforcement ratio.

The results for the high strength concrete are obtained by using the same values of w_c and β as for

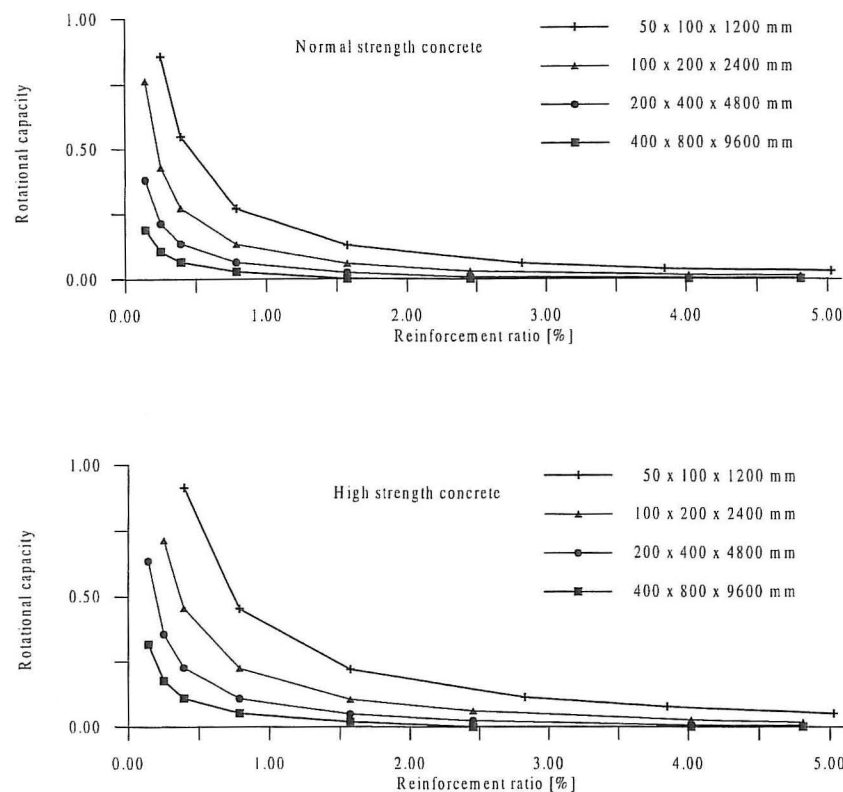


Figure 5. Rotational capacity in the heavily reinforced regime. Top: Normal strength concrete. Bottom: High strength concrete.

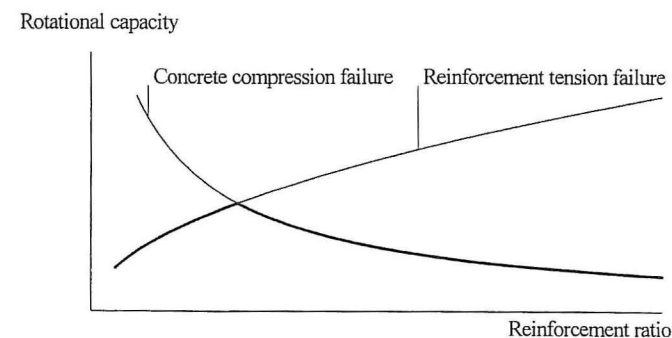


Figure 6. Combining models for lightly reinforced and heavily reinforced beams.

the normal strength concrete; only the compression strength and the failure strain (peak strain) have been increased. For higher strength concrete, there is no guarantee, that the key parameters w_c , β will be the same. In fact, experimental results (see Appendix D) indicate that a smaller value of w_c has to be used. However, keeping the key parameters the same, the results show a clear increase of the rotational capacity with strength.

The rotational capacity described by the model also depends weakly on the yield strength of the reinforcement just like the results of the model for the lightly reinforced regime described in the preceding subsection depends weakly on the tensile strength of the concrete. However, considering the two models defined above, the model for the lightly reinforced regime is describing rotational capacity mainly controlled by reinforcement tension failure, and the model for the heavily reinforced regime is describing rotational capacity mainly controlled by concrete compression failure. Now, Taking the smallest value of the rotational capacity predicted by the two models defines a model valid for all reinforcement ratios, the intersection point defining the transition from the failure mode where the rotational capacity is controlled mainly by reinforcement tensile properties to the failure mode where the rotational capacity is controlled mainly by concrete compression properties, see Figure 6.